Experimental and theoretical determination of rotational-translational state-to-state rate constants for N_2:He collisions at low temperature ($3<T<20$ K)

B. Maté[a)]
Instituto de Estructura de la Materia, CSIC, Serrano 121, 28006 Madrid, Spain

F. Thibault
Laboratoire de Physique des Atomes, Lasers, Molecules, et Surfaces (UMR-CNRS 6627), Universite de Rennes I, Campus de Beaulieu, F-35042 Rennes Cedex, France

A. Ramos, G. Tejeda, J. M. Fernández, and S. Montero
Instituto de Estructura de la Materia, CSIC, Serrano 121, 28006 Madrid, Spain

(Received 7 November 2002; accepted 16 December 2002)

We present an experimental determination of state-to-state rotational–translational (RT) rate constants of N_2:He collisions in the vibrational ground state as a function of temperature in the range $3<T<20$ K. Raman spectroscopy in supersonic expansions of N_2/He mixtures is used to determine the primary data that, together with the N_2:N_2 state-to-state RT rates previously determined [Ramos *et al.*, Phys. Rev. A **66**, 022702 (2002)], are needed to solve the master equation according to a procedure that does not impose any particular scaling law. We also report first principle calculations of the N_2:He state-to-state RT rate constants performed using the full three-dimensional potential energy surface of Reid *et al.* [J. Chem. Phys. **107**, 2329 (1997)], in the $3<T<300$ K temperature range. The coupled-channel method, and the coupled-states approximation, were applied in the low (0–610 cm^{-1}) and in the high (610–1500 cm^{-1}) energy limits, respectively. A good agreement between theoretical and experimental results is found in the temperature range where comparison is possible. © *2003 American Institute of Physics.*
[DOI: 10.1063/1.1543945]

I. INTRODUCTION

Molecular inelastic collisions affect a wide range of phenomena in gases, as for instance, diffusion, viscosity, heat conductivity, broadening of spectral lines, rotational relaxation, breakdown of thermodynamic equilibrium in supersonic jets, shock waves properties, and others. The study of rotational–translational (RT) energy transfer in collisional processes and, in particular, the determination of the state-to-state collisional rate constants, enhances the understanding of elementary collision dynamics, bridges the microscopic–macroscopic interphase in fluid mechanics, and provides valuable information on the potential-energy surfaces (PES) of molecular interactions.

The first experimental studies of rotational relaxation of molecules were mainly bulk phase experiments. Macroscopic quantities like rotational relaxation time, τ_R, or average rotational relaxation cross sections, σ_R, were determined, but restricted to room temperature.[1] In particular, the rotational energy transfer between nitrogen molecules and noble gas atoms was studied intensively by Kistemaker and Vries.[2] Using acoustic techniques they studied the rotational relaxation of N_2 by He, Ne, Ar, and Xe, and found the trend Ne>Ar>Xe>He for relaxing efficiency of the different colliding partners at room temperature.

In the last decades, free jets or molecular beam experiments, combined with spectroscopic techniques, have been applied to derive the low temperature dependence of those macroscopic quantities. Electron-beam induced fluorescence,[3–5] resonance-enhanced multiphoton ionization (REMPI),[6,7] or stimulated Raman spectroscopy[8] provide rotational populations of the molecular levels that have been used to determine the average relaxation cross sections. These macroscopic quantities contain integrated information of the individual state-to-state rate constants. The state-to-state rates can, in principle, be derived from them in an indirect way using a scaling model and an inversion procedure.

Measurements of self-broadening coefficients of spectral lines by high resolution spectroscopy have provided information about state-to-state rate constants at room temperature and above for systems like N_2 (Ref. 9) or C_2H_2–He.[10] Rotational distributions in free jets, measured by different laser spectroscopic techniques, have also been used to obtain these state-to-state rate constants in systems like CO–He,[11] HF–He,[12] CO–Ar,[13] CS_2–Ar,[14] or N_2–N_2.[15] However, in these works, some kind of empirical scaling law was imposed to relate the different state-to-state rate constants. So far, the most straightforward experimental method to determine state-to-state collisional rate constants is based in populating selected rotational levels by stimulated Raman-pumping,[16] but this technique provides information only about rotational states within the $v=1$ vibrational state, and is difficult to apply below room temperature. For the rotational ground state ($v=0$) and low temperature the ex-

[a)]Electronic mail: b.mate@iem.cfmac.csic.es

perimental methodology presented in a previous paper[17] is a promising alternative. It will be applied in this work to determine experimentally the relevant state-to-state rate constants for N_2:He collisions in the low temperature range of $3<T<20$ K. In this methodology, based on Raman spectroscopic data measured from supersonic expansions of N_2/He mixtures, neither a scaling law is imposed among the rate constants, nor a special model is required to describe the flow properties. To compare with we also present calculated RT state-to-state rate constants for N_2:He collisions in the temperature range $3<T<20$ K. These calculations, which span the thermal range up to 300 K, were performed using the full three-dimensional (3D) potential energy surface (PES) of Reid *et al.*[18]

Present paper is structured as follows: The experimental methodology used to obtain the RT state-to state rate constants is described in some detail in Sec. II. Section III is devoted to the experimental system. Then, we present and discuss the experimental results in Sec. IV. Section V is dedicated to first principle calculations of the N_2:He RT rate constants, and Sec. VI to compare our theoretical and experimental results. In Sec. VII the N_2:He average cross sections for relaxation of the mean rotational energy at various temperatures are derived from our theoretical calculations and experimental state-to-state rates, and are compared with previous results from the literature. Finally, a summary and the main conclusions are presented in Sec. VIII.

II. METHODOLOGY

Steady supersonic expansions are easily produced in the laboratory by expanding the sample gas through a small circular nozzle (diameter <1 mm) into a chamber maintained at low pressure (<1 mbar). In such expansions the remarkable properties are: (1) supersonic flow velocity (V), (2) fast decrease of number density (n), and (3) sharp cooling, down to a few kelvin, with progressive breakdown of thermal equilibrium ($T_t \neq T_r$) between translational (T_t) and rotational (T_r) temperature. This breakdown is due to the collisional deficit associated with the increasing rarefaction of the expanding gas. It plays a central role in the present method, and will be described here quantitatively in terms of a local nonequilibrium parameter X defined in the following.

The present method relies exclusively on the experimental data derived from the rotational and vibrational intensities of linear Raman spectra recorded at consecutive points along the axis of a steady supersonic expansion of a molecular gas. Each of these points represents, by virtue of the distance (z) from the beginning of the expansion, a gas volume at different time (t). Since position z and time t are related in the jet by the flow velocity, a quantity that can be determined from experimental data, the ensemble of spectra recorded at the different points of the expansion contains the information about the kinetics of the rotational population, and about the rate constants, as has been recognized long ago.[11,12]

The theoretical basis of the method is the master equation[19] that describes the energy transfer between rotational and translational degrees of freedom considering explicitly the discrete nature of rotational levels. This equation, expressed for a gas of identical diatomic molecules, has the form:

$$\frac{dP_i}{dt} = n \sum_{j,l,m} (-P_i P_j k_{ij\to lm} + P_l P_m k_{lm\to ij}), \tag{1}$$

where dP_i/dt is the time derivative of the normalized population P_i, $(\Sigma_i P_i = 1)$, of a rotational energy level with quantum number $J=i$, and $n(t)$ is the instantaneous number density of molecules in the gas with translational temperature $T_t(t)$. Indices i, j, l, m span the domain of the rotational quantum number J of the diatomic molecule; $k_{ij\to lm}$ are the state-to-state rotational–translational rate constant for the elementary collisional process between two molecules. In the case of N_2:N_2 collisions, $k_{ij\to lm}$ describes the rate of the elementary process:

$$N_2(i) + N_2(j) \xrightarrow{k_{ij\to lm}} N_2(l) + N_2(m), \tag{2}$$

between a N_2 molecule (active) in rotational state $J=i$ and another N_2 molecule (passive) in the rotational state $J=j$. Recent calculations on H_2 collisions[20] show that the $k_{ij\to lm}$'s are quite insensitive to the rotational state of the passive molecule. This suggests the use of the reduced rates k_{il} as a reasonable approximation. Under this hypothesis the reduced rates become defined by the relation $k_{ij\to lj} = S_{ijlj} k_{il}$, with $S_{ijlj} = (1+\delta_{ij}\delta_{lj})/(1+\delta_{ij})(1+\delta_{lj})$,[19] in order to avoid double counting of some collisions between indistinguishable molecules. In terms of the reduced rates, the master equation for collisions between identical N_2 molecules becomes

$$\frac{dP_i}{dt} = n \left(\sum_{j,l} (-P_i P_j k_{il} + P_l P_j k_{li}) \right) S_{ijlj}. \tag{3}$$

This equation was employed in a previous paper[17] for a detailed study of N_2:N_2 collisions. For a N_2/He mixture, in addition to N_2:N_2 pairs, N_2:He collisions have to be taken into account, with their corresponding rotational–translational rate constants associated with the elementary process

$$N_2(i) + He \xrightarrow{h_{i\to l}} N_2(l) + He. \tag{4}$$

In this case, only indices i and l are required, since helium has no rotational states. N_2:He rate constants will be referred to as h_{il}, in order to distinguish them from the N_2:N_2 rates. For N_2/He mixtures, the master equation must include two terms, describing the two different kinds of collisions or elementary processes, N_2:N_2 and N_2:He, respectively. In a general case of a N_2/He mixture with a molar fraction α of N_2 molecules, the master equation will then be

$$\frac{dP_i}{dt} = n \left[\alpha \sum_{l,j} (-P_i P_j k_{il} + P_l P_j k_{li}) S_{ijlj} + (1-\alpha) \sum_{l} (-P_i h_{il} + P_l h_{li}) \right]. \tag{5}$$

For our purposes, it is convenient to transform the master equation from the time domain into the spatial domain.

The evolution of the rotational populations of N_2 along the expansion axis for a stationary free jet can this way be expressed as

$$\frac{dP_i}{d\tilde{z}}\frac{V}{D}=n\left[\alpha\sum_{l,j}(-P_iP_jk_{il}+P_lP_jk_{li})S_{ijlj}+(1-\alpha)\sum_{l}(-P_ih_{il}+P_lh_{li})\right], \quad (6)$$

where $\tilde{z}=z/D$, z being the distance from the nozzle, and D the nozzle diameter; $V(z)=dz/dt$ is the instantaneous local flow velocity of the gas mixture. Making use of the microscopic reversibility principle and assuming that rotational populations are properly described by a rotational temperature T_r, as we observe in the zone of silence of the expansions studied here, the right-hand term of Eq. (6) can be simplified and expressed as

$$\frac{dP_i}{d\tilde{z}}\frac{V}{D}=\alpha\left[\sum_{r<i}(-a_{ri}k_{ri})+\sum_{s>i}(a_{is}k_{is})\right]+(1-\alpha)\left[\sum_{r<i}(-c_{ri}h_{ri})+\sum_{s>i}(c_{is}h_{is})\right], \quad (7)$$

where the constants k_{il} and h_{il} always refer to upward transitions ($i<l$). The coefficients a_{il},

$$a_{il}=nP_i\left(1-\frac{P_i+P_l}{2}\right)[-1+e^{[l(l+1)-i(i+1)]X}], \quad (8)$$

were given in our previous paper;[17] the factor $1-(P_i+P_l)/2$ takes into account the effect of collisions between indistinguishable N_2 molecules. $X=\beta B(T_t^{-1}-T_r^{-1})$ is the local nonequilibrium parameter, where $\beta=hc/k_B=1.4388$ K/cm^{-1}, and $B=1.989\,73$ cm^{-1} is the rotational constant of N_2. The coefficients c_{il} are given by

$$c_{il}=nP_i[-1+e^{[l(l+1)-i(i+1)]X}]. \quad (9)$$

Since natural N_2 is a 2:1 mixture of *ortho*- ($i=J=$even) and *para*- ($i=J=$odd) noninterconverting species, the master equation (7) may be split into two independent subsystems. Each subsystem will reflect the property

$$\sum_{i=\text{even}}\frac{dP_i}{dt}=0, \quad \sum_{i=\text{odd}}\frac{dP_i}{dt}=0, \quad (10)$$

respectively, which arise from the conservation of *ortho*- and *para*-N_2 normalized populations $\Sigma_{i=\text{even}}P_i=2/3$, and $\Sigma_{i=\text{odd}}P_i=1/3$.

In master equation (7) the independent terms $dP_i/dt=(dP_i/d\tilde{z})(V/D)$, and the coefficients a_{il}, c_{il}, are quantities that can be determined from experimental data as explained in the following. Since rotational–translational rates k_{il} for N_2: N_2 are known from our previous work[17] the only unknown parameters in Eq. (7) are the N_2:He rate constants, h_{il}.

Solving the two subsystems derived from Eq. (7), for *ortho*-N_2 and *para*-N_2, to obtain the even and odd rates h_{il} is not immediate due to their peculiar structure. In principle, we have an infinite number of equations but, at a given temperature, only a finite number of them are meaningful. At $T_t<20$ K just equations up to dP_4/dt and dP_5/dt were retained for *ortho*- and *para*-N_2, respectively. A more difficult point is, in principle, the infinite number of unknowns h_{il} in Eq. (7). A common procedure to circumvent this problem is to assume a so-called "scaling law," which provides relations between different h_{il}'s as a function of temperature by means of a reduced number of parameters. Although there is general agreement that scaling laws should involve exponential functions of $\epsilon_{il}=(E_l-E_i)/(k_BT_t)$, for $|E_l-E_i|$ the rotational energy change in the collision, none of the models checked in the literature for N_2:He system extends to the low temperatures investigated in this work. Thus, instead of using a particular scaling law, we apply the less restrictive condition, common to all of them,

$$0<h_{i'l'}<h_{il}$$

if

$$(E_l-E_i)<(E_{l'}-E_{i'}), \quad (11)$$

holding separately for *ortho*- and *para*-subsystems. Combining these constraints with the system of meaningful equations, the resulting linear system can be solved using a linear programming method, where a mean-square solution can be found for the relevant h_{il}'s.

III. EXPERIMENTAL SYSTEM

The experimental system used for the present measurements has been described elsewhere[21] and only the relevant details will be given here. Two continuous free jets of N_2/He mixtures (molar fractions of N_2 $\alpha=0.47$ and 0.076) were generated by expanding the gas mixtures through a circular nozzle of diameter $D=313$ μm. Stagnation temperature was $T_0=296$ K, and stagnation pressure was maintained constant at $P_0=1$ bar. The gas was expanded into a 130 l low pressure chamber pumped out by a 2200 l s^{-1} turbomolecular pump, backed by a roots and a rotatory pump of 400 and 70 m^3/h, respectively. Under these conditions the low pressure chamber reaches a residual pressure of about 0.01, and 0.02 mbar, for expansions with $\alpha=0.47$ and 0.076, respectively. The different residual pressures are due to the different efficiency of the pumps for N_2 and He.

A Beamlock 2080 Spectra Physics Ar^+ laser source was used for excitation of Raman scattering. Typical excitation power was 6 W at $\lambda=514.5$ nm, with the laser beam sharply focused with a lens of $f=35$ mm in a beam waist of ≈ 14 μm. The Raman spectrometer, a noncommercial instrument commissioned in our laboratory,[22] is equipped with a 2360 lines/mm holographic grating of 102×102 mm^2 as dispersive element, and a 1340×400 charge coupled device (CCD) detector (Princeton Instruments LN/CCD-1340/400-EB/1) refrigerated by liquid N_2, that provides a very high sensitivity. CCD bidimensional detection in connection with the sharply focused laser beam leads to a working spatial resolution of a few microns on the jet. For better stability the laser beam is kept fixed and the nozzle is moved in order to record Raman spectra at different points along the axis of the supersonic expansions. Axial motion is controlled by an optically codified micropositioner with precision of ±1 μm.

Absolute accuracy of the axial distance between the nozzle and the observed region is ± 10 μm. Errors in the reduced distance $\tilde{z}=z/D$ appearing in Eq. (7) are therefore negligible.[23,24]

The region of interest for relaxation studies is within the zone of silence of the axisymmetric supersonic expansions, spanning the range $6D<z<30D$ for expansion with $\alpha=0.47$, and $3D<z<13D$ for expansion with $\alpha=0.076$. Positions closer to the nozzle exit are affected by turbulences in the flow. Far end limits are imposed by the onset of the normal shock wave (Mach disk) of the expansions.

Rotational and vibrational Raman spectra of the N_2 species in the expanded N_2/He mixtures were recorded at different z points along the expansion axis. From these measurements the total number densities n and the rotational populations P_i appearing in Eqs. (8) and (9) were determined as detailed next. Relative number densities of N_2 were measured from the integrated Raman intensity of the Q branch of the vibrational band of N_2 at 2331 cm^{-1}. To a very good approximation this Raman intensity,

$$I_{2331}=K\times n, \tag{12}$$

is proportional to the local number density n at the observed spot in the medium. For temperatures below 300 K the factor K only depends on exciting irradiance and wavelength, scattering geometry, and molecular polarizability derivative of N_2, magnitudes that remain constant along the experiment. The relative number densities can be converted to absolute values by comparison with a reference medium of known number density. In the present case, this absolute calibration was carried out at selected points of the expansions comparing the Raman signal of N_2 (Q branch at 2331 cm^{-1}) with the corresponding signal from static N_2 at $P=10$ kPa and $T=295$ K. He atoms cannot be detected by Raman spectroscopy. For that reason, to determine the absolute number density of He we make use of the experimentally determined molar fraction α of N_2 in the mixtures, a quantity accurate to about 1%. The absolute total number density n of the N_2/He mixtures is determined with an accuracy of about 14%.

Populations P_J of the rotational levels of N_2 were measured from the relative intensities of the rotational lines of the Raman spectra of N_2. The intensities of the rotational lines associated with $J\rightarrow J+2$ Raman transitions of linear molecules may be expressed as

$$I_{J\rightarrow J+2}=GP_J\frac{(J+1)(J+2)}{(2J+1)(2J+3)}. \tag{13}$$

Factor G depends on exciting irradiance and wavelength, scattering geometry, and anisotropy of the molecular polarizability, and remains constant along the experiment. P_J's were measured as a function of $\tilde{z}$ from the $I_{J\rightarrow J+2}$ intensities of the rotational spectra of N_2 spanning the range between 5 and 180 cm^{-1}. For levels up to $J=5$ no significant deviation from a Boltzmann distribution was observed and a rotational temperature $T_r(z)$ was assigned to each z point with an estimated accuracy of ± 0.2 K, for $T_r<30$ K.

In the present context it can be affirmed that linear Raman spectroscopy provides, among the other spectroscopic techniques, the most direct and accurate measurement of absolute densities and rotational populations along a free jet, signal being linear with density along several orders of magnitude.[21]

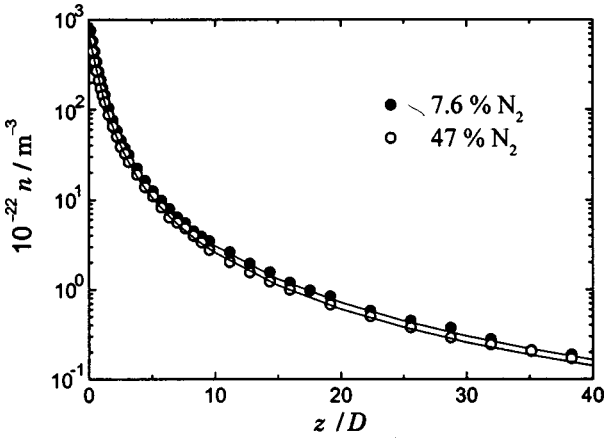

FIG. 1. Experimental absolute total number density along the axis of N_2/He expansions. Nozzle diameter $D=313$ μm. Solid lines represent analytical fits.

IV. EXPERIMENTAL RESULTS

The absolute total number densities $n(z)$ measured along the expansion axis are shown in Fig. 1. The corresponding rotational temperatures are shown in Fig. 2. In Figs. 1 and 2 solid lines represent the smoothing of the experimental data by means of suited analytical functions. These smoothed data have been used here as the primary data to obtain the N_2:He collisional rate constants. In Fig. 1 a faster density decay along the expansion axis is observed for the expansion with higher molar fraction of N_2. The averaged specific heat ratio γ that describes the gas mixture is $\gamma=1.533$ for $\alpha=0.47$, and $\gamma=1.648$ for $\alpha=0.076$. Macroscopic fluid dynamic models, like the isentropic model, predict a faster density decay for gases with lower gamma values, in agreement with present experimental results.

The rotational temperatures shown in Fig. 2 are lower for expansion with $\alpha=0.076$ than for expansion with $\alpha=0.47$. This behavior can be understood in terms of the molar fractions, α, and of the difference between the rates k_{il}

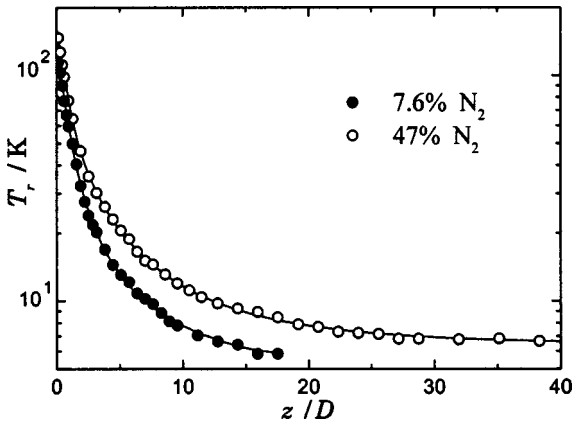

FIG. 2. Experimental rotational temperature along the axis of N_2/He expansions. Nozzle diameter $D=313$ μm. Solid lines represent analytical fits.

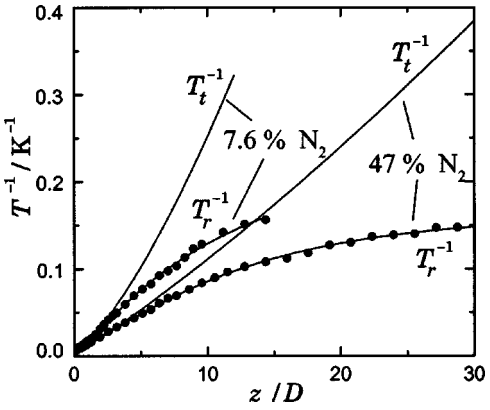

FIG. 3. Inverse rotational and translational temperatures along the axis of N_2/He expansions. Nozzle diameter $D=313$ μm.

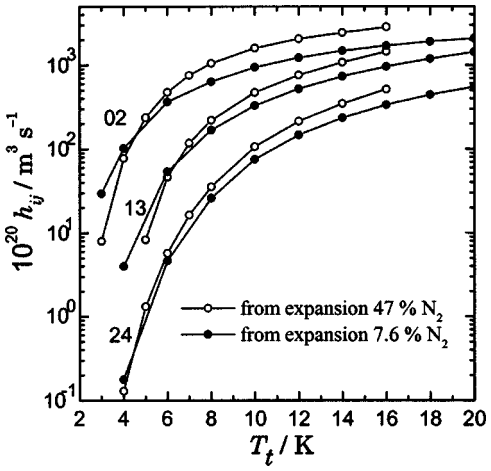

FIG. 4. Experimental state-to-state rate constants h_{il} of N_2:He collisions vs translational temperature T_t.

for N_2:N_2 collisions and h_{il} for N_2:He collisions. The two right-hand terms in the master equation (7) refer to these two contributions. For expansion with $\alpha=0.47$ both terms contribute in a comparable amount to the variation of rotational populations. For expansion with $\alpha=0.076$, the contribution of the second term involving N_2:He collisions dominates the evolution of the rotational population of N_2. The data set summarized in Figs. 1 and 2, and given in detail in TABLE-H.TXT,[25] contains the information about collisional rates in N_2/He mixtures. To extract this information according to the above-outlined procedure, Eqs. (7)–(9), the translational temperatures $T_t(z)$ and the flow velocities $V(z)$ are also needed. The procedure to obtain these quantities from the experimental data has been described in a previous work,[26] and will be adapted here to mixtures.

In order to determine T_t and V in a gas mixture the following averaged quantities must be defined: the averaged rotational heat capacity at constant pressure for the N_2/He gas mixtures, which is given to a good approximation by $\langle C_{P,r}\rangle=\alpha C_{P,r}^{N_2}$, and the averaged molar mass of the mixture given by $\langle W\rangle=\alpha W^{N_2}+(1-\alpha)W^{He}$; $C_{P,r}^{N_2}=R$ is the rotational heat capacity of N_2, $R=8.3145$ J K^{-1} mol^{-1} the universal gas constant, and $W^{N_2}=0.028$ kg/mol and $W^{He}=0.004$ kg/mol, the molar masses of N_2 and He, respectively. These approximations imply considering the free jet of the mixture equivalent to a pure molecular gas free jet with the averaged gas properties $\langle C_{P,r}\rangle$ and $\langle W\rangle$. Imposing conservation of momentum and total enthalpy along the expansion axis, translational temperature, rotational temperature, and number density along the expansion are related by the differential equation[26]

$$\frac{dT_t}{dz}=\frac{2}{3}\left[\frac{1}{n}\frac{dn}{dz}T_t-\alpha\frac{dT_r}{dz}\right]. \tag{14}$$

By solving this differential equation for the initial condition of thermodynamic equilibrium, $T_r=T_t$, near the expansion origin, the translational temperature $T_t(z)$ along the expansion axis is obtained. The inverse of the translational temperatures obtained this way is shown in Fig. 3, together with the inverse of the rotational temperatures, in order to help visualizing the breakdown of rotational–translational equilibrium. We have estimated a 2% error in T_t, mainly due to propagation of α, $n(z)$, and $T_r(z)$ experimental errors, and to the initial condition chosen. In the unperturbed regions, $6D<z<30D$ for expansion with $\alpha=0.47$, and $3D<z<13D$ for expansion with $\alpha=0.076$, the translational temperatures range from 20 to 3 K.

From the total enthalpy conservation the flow velocity, $V(z)$, for a He/N_2 mixture is given by

$$\langle V(z)\rangle=\left[\frac{R}{\langle W\rangle}((5+2\alpha)T_0-5T_t(z)-2\alpha T_r(z))\right]^{1/2}, \tag{15}$$

where T_0 is the source temperature. We have estimated an error of 1% in the determination of this quantity. The uncertainty in $\langle V(z)\rangle$ just mentioned only considers errors in n, α, T_r, and T_t, and do not take into account errors implicit in the approximations deriving from averaging heat capacities and molar masses. A listing with the numerical values of n, T_r, T_t and V is given in TABLE-H.TXT.[25] The smoothed values in TABLE-H.TXT are given with a number of digits higher than the actual experimental accuracy in order to avoid round off errors in the calculations.

At this point, the primary data given in TABLE-H.TXT are used as input for implementing the procedure described in Sec. II. First, coefficients a_{il} and c_{il} defined in Eqs. (8) and (9) are determined using the values of T_r, T_t, and n. These coefficients, together with the N_2:N_2 rate constants k_{ij} given in our previous work,[17] are introduced in the master equation (7). Then, the two systems of master equations for *ortho*- and *para*-N_2 species are solved to obtain a set of h_{il} rate constants for N_2:He collisions. This way we have obtained the rate constants h_{02}, h_{13}, h_{24}, h_{35}, h_{04}, h_{15}, h_{46}, h_{26}, and h_{06}, in the temperature range $3<T_t<20$ K. Some of the h_{il} determined for both expansions are shown in Fig. 4. In the thermal range studied here we found empirically that they obey, to a good approximation, an exponential law

$$h_{il}=C_{il}e^{-b_{il}\epsilon_{il}}, \tag{16}$$

where $\epsilon_{il}=(E_l-E_i)/k_BT_t$. The coefficients C_{il} and b_{il}, averaged over both expansions, are presented in Table I together with their estimated uncertainties.

TABLE I. Coefficients C_{il} and b_{il} for the rate constants h_{il} (N_2:He collisions), and k_{il} (N_2:N_2 collisions), determined experimentally in the range $3<T_t<20$ K.

	h_{il} (this work)		k_{il} (Ref. 17)	
il	b_{il} dimensionless	$10^{20}C_{il}$ (m^3/s)	b_{il} dimensionless	$10^{20}C_{il}$ (m^3/s)
02	0.958±0.031	6699±1701	0.886±0.010	10 900±850
13	1.026±0.049	7741±2196	0.920±0.015	8210±450
24	1.048±0.027	6227±1461	0.988±0.018	8930±260
35	1.078±0.017	9590±3251	0.948±0.016	5600±50
04	0.808±0.004	3865±675	0.865±0.031	7050±750
15	0.916±0.021	5384±2026		
46	0.947±0.016	3535±453	0.971±0.018	4580±1200
26	0.892±0.007	3546±467	0.964±0.055	8150±1800
06	0.813±0.016	1965±116		

Due to the very low population of the rotational levels with $J>4$ at $T_r<20$ K, the rates h_{02} and h_{13} are determined best, while h_{24}, h_{35}, h_{04}, h_{15}, h_{26}, etc., have increasingly larger uncertainties. Collisional rate constants h_{il} only depend on the translational temperature of the medium, i.e., on the collisional energy, and are expected to be invariant with respect to the number density and the rotational temperature. So, the differences observed between the two sets of rate constants, $h_{il}(\alpha=0.47)$ and $h_{il}(\alpha=0.076)$, in Fig. 4, are not physically meaningful. The two set of constants differ, in the worst cases, by 30%. These differences reflect mainly the experimental uncertainties and also the validity of the different approximations imposed. The experimental error is propagated from $n(z)$ and $T_r(z)$, the quantities directly measured, to $T_t(z)$ and to the a_{il} and c_{il} coefficients of Eqs. (8) and (9). These coefficients depend exponentially on the local nonequilibrium parameter $X(z)=\beta B(T_t^{-1}-T_r^{-1})$. The larger the difference $T_t^{-1}-T_r^{-1}$, the more accurately it can be measured, and the more precisely the c_{il} and a_{il} coefficients can be determined. As shown in Fig. 3, $X(z)$ tends to zero near the beginning of the expansion, the region of higher rotational and translational temperatures and densities, and therefore, the region of higher collisional activity. We estimate a 25% experimental error for the h_{il}'s in the 20 K translational temperature region, decreasing for lower temperatures. Another source of indetermination is the 30% uncertainty estimated in the N_2:N_2 RT rate constants, k_{il}, studied in our previous work,[17] that are used here for the determination of the h_{il} constants. The effect will be stronger in expansion with $\alpha=0.47$ than in expansion with $\alpha=0.076$, and we have estimated that it represents less than a 20% uncertainty in the h_{il}'s determined here.

Other sources of uncertainty may arise from the method used to obtain the flow properties T_t and V. Imposed momentum and enthalpy conservation laws along the expansion axis is a safe assumption but, to obtain T_t and V along the free jet, averaged rotational heat capacity and mass weight were defined. These approximations lead to an averaged flow velocity and may imply some error since lighter particles tend to flow faster than heavier ones in free jets, the so-called slip effect.[27] Another effect, well established for supersonic expansions of gas mixtures, is that the heavier species tend to focus in the expansion axis while the lighter ones move away from it.[28] This might cause a change in concentration along the expansion axis that has not been considered in our treatment. Thus, it is difficult to determine how much the above-mentioned approximations can affect the final results. In any case, the deviation observed between the two set of constants $h_{il}(\alpha=0.47)$ and $h_{il}(\alpha=0.076)$, which in principle should be identical, reflects empirically the uncertainty level of our results.

As far as we know, no experimental data have been reported in the literature for state-to-state RT rate constants of N_2:He collisions in this temperature range. Only some calculations of state-to-state cross sections were found (see Fig. 5) but not at temperatures below 20 K. Therefore we can only compare with our theoretical results.

V. FIRST PRINCIPLE CALCULATIONS

The first principle calculations of the h_{il} rate constants defined and measured above were performed using the full 3D PES of Reid *et al.*,[18] fixing the N_2 bond length at his equilibrium value $r_e=2.0743\ a_0$. This PES is thought[18,29] to be sufficiently accurate to predict correctly a large variety of experimental data.[30] In particular this PES has been successfully tested[18] against experimental rate constants for the deactivation of N_2 ($v=1$) by He for temperatures down to 50 K. To provide the rotational state-to-state cross sections σ_{ij},

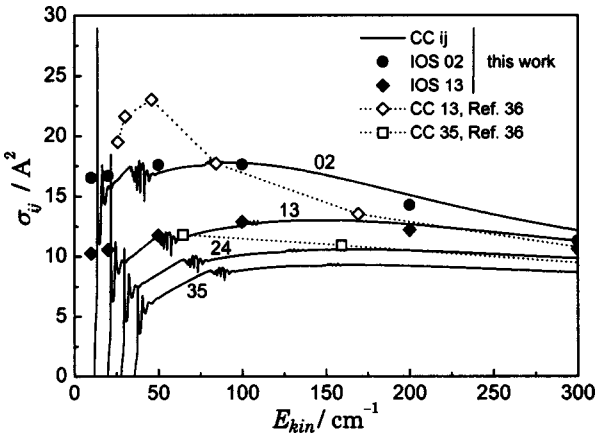

FIG. 5. Calculated upward state-to-state cross sections σ_{il} of N_2:He collisions vs collision energy.

at a given total energy (E_T), both MOLCOL[31] and MOLSCAT[32] scattering codes were used for convenience. In the interval $0<E_T<610$ cm^{-1} the scattering computations were done with MOLCOL using the coupled channel (CC) method, whereas for higher energies, up to 1500 cm^{-1}, MOLSCAT was used in conjunction with the coupled states (CS) approximation.[33] A few CC calculations were also done with MOLSCAT code at lower energies to check that the transition from one code to the other was smooth enough. In order to solve the coupled equations the propagation is carried out from 3 to 50 a_0 with a constant step size corresponding approximately to about 12 points per half wavelength associated with the sum of the total energy and the maximum well depth (20 cm^{-1}). In fact, the step size varied accordingly with the energy in order to accurately probe the well of the PES. This was achieved with MOLCOL using the Johnson log-derivative propagator,[34] while the hybrid log-derivative/Airy propagator[35] was used with MOLSCAT. In the latter case the switch from the log-derivative to the Airy propagator was held fixed at an intermolecular distance of 25 a_0. The *ortho*- and *para*-N_2 species were treated independently. In addition to the energetically open rotational levels of N_2, five closed levels were included in the basis set in case of the CC method, and many more in the CS method. The energies of N_2 rotational levels were generated with a rotational constant $B_0=1.989\,59$ cm^{-1}. The PES was projected onto nine Legendre polynomials from P_0 to P_{16} with the help of a 20-points-Gauss Legendre quadrature. The masses of the colliding pairs are: $m(N_2)=28.006\,148$ and $m(\mathrm{He})=4.002\,602$ u, with a reduced mass of $\mu=3.5026$ u. The summation over the partial waves was stopped when the elastic probability in the $J=0$ (or $J=1$ for *para*-N_2) converged to better than 10^{-4}; this gives a relative error for this cross section of the order of 0.5% and much smaller for the inelastic cross sections. For example at total energies of 25, 100, and 610 cm^{-1}, respectively, 22, 41, and 73 partial waves were included for a run of MOLCOL. Overall, due to the truncation in the basis set, the range and the step size of integration, and the number of partial waves included, state-to-state cross sections are expected to converge to better than 1% at each total energy. In order to obtain accurate rate constants in the investigated low temperature range, cross sections were calculated over a fine grid of energies. Between 11.9 and 100 cm^{-1}, where resonances are noticeable,[36] essentially near each rotational threshold (see Fig. 5), a step size in energy of 0.1 cm^{-1} was used. For higher energies and up to 610 cm^{-1} this step size was increased regularly from 0.2 to 20 cm^{-1}. The additional CS calculations were performed for energies of 650, 700, 800, 1000, and 1500 cm^{-1}. Figure 5 shows the CC upward state-to-state cross sections $\sigma_{ij}(E_{\mathrm{kin}})$, up to $E_{\mathrm{kin}}=300$ cm^{-1}; $E_{kin}=E_T-E_i$ is the available precollisional kinetic energy in a $J=i$ rotational level, for the rotational quantum numbers $J=0$, 1, 2, and 3.

The rate constants for N_2:He collisions, $h_{ij}(T)$, were obtained from the rotational cross sections as

$$h_{ij}(T)=\langle v\rangle \frac{1}{(k_BT)^2}\int_{E_s}^{\infty}\sigma_{ij}(E_{\mathrm{kin}})\exp\left(-\frac{E_{\mathrm{kin}}}{k_BT}\right)E_{\mathrm{kin}}dE_{\mathrm{kin}}, \tag{17}$$

by assuming the colliding particles to obey a Maxwellian thermal distribution at a temperature T. E_s is the minimum kinetic energy for the level $J=j$ to be accessible and $\langle v\rangle=((8k_BT)/(\pi\mu))^{1/2}$ is the mean relative velocity of the colliding partners. Downward as well as upward collisional rates were calculated with help of Eq. (17) in the temperature range 0–300 K. For this purpose three quadrature routines were used. A first routine computes the integral of a cubic spline form (NAG routines E01BAF+E02BDF), a second quadrature is performed with the D01GAF NAG's routine, and finally a simple trapezoidal rule is employed. Due to our fine grid of energies, relative errors between the different results provided by these quadrature procedures are less than 1%. Moreover, starting from one set of rate constants, downward or upward ones, upward and downward ones, respectively, are calculated through the detailed balance principle. Good consistency is found. These comparisons, as well as the errors on the state-to-state cross sections allow us to assert that our results are accurate to a few percent given the PES used. A summary of the more relevant rate constants at temperatures up to 300 K is given in Table II.

Several studies[36–40] were devoted to the average rotational relaxation cross sections[41] for N_2:He interactions. However, we only found in the literature the state-to-state cross sections σ_{ij} calculated by Thachuk and McCourt (see Figs. 8 and 12 in Ref. 36) which are easily comparable with ours (see Table 13.2 of Ref. 41). These authors used the so called HFD1 PES of Fuchs *et al.*,[42] without claiming that this PES was the most accurate available, to test the different methods[36,41] to calculate average rotational relaxation cross sections. Our findings, shown in Fig. 5, simply confirm the similarity of the upper part of the wall of the PES of Reid *et al.*[18] with the HFD1 PES, and the too strong anisotropy of the lower part of the latter PES.[39,43] Indeed, the HFD1 PES leads to a serious overestimation of the inelastic cross sections up to energies on the order of 100 cm^{-1}.

The effects of the resonances that appear at low kinetic energies has been thoroughly discussed.[18,36] The contribution of the resonances is more important at low temperature, and is also reinforced in the case of the σ_{02} as compared to the other cross sections because of the weighting function $E_{\mathrm{kin}}\exp(-E_{\mathrm{kin}}/k_BT)$. For instance, for the case of the σ_{02} rotational cross section we can roughly estimate the contribution of the resonances in the low temperature regime by deleting the two first peaks located just above the threshold of the $J=2$ level. These resonances account for 17%, 6.5%, and 4% to the rate at 5, 10, and 15 K, respectively.

VI. COMPARISON BETWEEN EXPERIMENTAL AND THEORETICAL RESULTS

In Fig. 6 we present a comparison between our experimental and theoretical results for N_2:He RT rate constants. On the whole, the agreement between experimental and first principle rates is encouraging. The experimental methodology developed to obtain the h_{il} rate constants solves numerically a system of master equations like Eq. (7). The uncertainties in the different quantities (n, T_r, T_t, V) that appeared in Eq. (7) do not affect in the same way the preci-

TABLE II. N_2:He calculated rate constants in $cm^3\,s^{-1}$. Notation: $2.932-12 \equiv 2.932\times10^{-12}$.

J_i	J_f	5	10	20	30	50	100	200	300 (kelvin)
0	2	2.932−12	1.687−11	4.294−11	6.167−11	8.771−11	1.229−10	1.502−10	1.625−10
0	4	2.227−16	7.224−14	1.481−12	4.555−12	1.313−11	3.698−11	7.160−11	9.128−11
0	6	1.544−22	2.770−17	1.397−14	1.319−13	1.022−12	7.308−12	2.697−11	4.464−11
0	8	1.051−30	1.024−21	3.898−17	1.617−15	4.434−14	9.883−13	7.986−12	1.854−11
0	10	7.499−41	3.772−27	3.318−20	8.699−18	1.117−15	9.543−14	1.940−12	6.721−12
0	12	4.532−53	1.272−33	8.488−24	2.069−20	1.674−17	6.910−15	4.028−13	2.095−12
2	4	2.559−14	1.403−12	1.062−11	2.160−11	4.027−11	7.106−11	1.036−10	1.216−10
2	6	1.885−20	5.830−16	1.121−13	7.118−13	3.587−12	1.540−11	3.930−11	5.725−11
2	8	1.340−28	2.272−20	3.382−16	9.611−15	1.748−13	2.329−12	1.240−11	2.439−11
2	10	1.002−38	8.821−26	3.077−19	5.601−17	4.856−15	2.488−13	3.190−12	9.095−12
2	12	6.390−51	3.130−32	8.327−23	1.422−19	7.874−17	1.938−14	6.927−13	2.972−12
4	6	2.426−16	1.335−13	3.203−12	9.558−12	2.398−11	5.152−11	8.173−11	9.963−11
4	8	1.937−24	5.865−18	1.105−14	1.490−13	1.356−12	8.771−12	2.675−11	4.156−11
4	10	1.592−34	2.508−23	1.119−17	9.777−16	4.299−14	1.069−12	7.496−12	1.615−11
4	12	1.097−46	9.633−30	3.305−21	2.733−18	7.775−16	9.301−14	1.745−12	5.592−12
6	8	2.137−18	1.180−14	9.080−13	4.036−12	1.408−11	3.879−11	6.885−11	8.666−11
6	10	1.955−28	5.630−20	1.036−15	3.004−14	5.075−13	5.227−12	1.981−11	3.284−11
6	12	1.496−40	2.401−26	3.419−19	9.448−17	1.043−14	5.140−13	4.973−12	1.182−11
8	10	1.936−20	1.034−15	2.501−13	1.648−12	8.009−12	2.887−11	5.879−11	7.727−11
8	12	1.592−32	4.748−22	8.962−17	5.675−15	1.812−13	3.060−12	1.489−11	2.675−11
10	12	1.496−22	8.361−17	6.607−14	6.512−13	4.435−12	2.112−11	5.005−11	6.931−11
1	3	2.594−13	4.527−12	1.968−11	3.365−11	5.535−11	8.950−11	1.224−10	1.387−10
1	5	1.865−18	5.891−15	3.689−13	1.631−12	6.255−12	2.232−11	5.135−11	7.091−11
1	7	1.301−25	7.146−19	1.950−15	3.193−14	3.807−13	3.799−12	1.746−11	3.208−11
1	9	9.125−35	8.459−24	3.082−18	2.679−16	1.311−14	4.514−13	4.765−12	1.255−11
1	11	6.080−46	9.595−30	1.471−21	9.851−19	2.634−16	3.879−14	1.087−12	4.296−12
3	5	2.515−15	4.369−13	5.870−12	1.440−11	3.095−11	5.974−11	9.080−11	1.090−10
3	7	1.937−22	5.905−17	3.537−14	3.260−13	2.193−12	1.145−11	3.183−11	4.804−11
3	9	1.467−31	7.582−22	6.165−17	3.063−15	8.615−14	1.553−12	9.443−12	1.949−11
3	11	1.042−42	9.207−28	3.187−20	1.234−17	1.929−15	1.496−13	2.306−12	6.979−12
5	7	2.300−17	4.004−14	1.719−12	6.254−12	1.846−11	4.472−11	7.474−11	9.246−11
5	9	1.965−26	5.799−19	3.412−15	6.741−14	8.341−13	6.776−12	2.292−11	3.670−11
5	11	1.538−37	7.790−25	1.969−18	3.059−16	2.127−14	7.415−13	6.074−12	1.371−11
7	9	2.050−19	3.511−15	4.786−13	2.590−12	1.066−11	3.355−11	6.362−11	8.171−11
7	11	1.745−30	5.160−21	3.056−16	1.311−14	3.045−13	4.009−12	1.717−11	2.958−11
9	11	1.665−21	2.912−16	1.282−13	1.035−12	5.965−12	2.473−11	5.427−11	7.315−11

sion of the final results. Due to the exponential dependence of the c_{il} coefficients in Eq. (9) on the nonequilibrium parameter $X=\beta B(T_t^{-1}-T_r^{-1})$ small errors in the translational temperatures critically affect the final h_{il} obtained. At high translational temperatures the parameter X tends to zero and the c_{il} coefficients have a larger uncertainty. For that reason the experimental rate constants h_{il} obtained are better determined at 4 that at 20 K. The fact that the present experimental h_{il} agree well within the order of magnitude with our first principle calculations constitutes an indirect validation of those previously determined experimental k_{il} for $N_2:N_2$, and of the experimental methodology itself. Comparison between experimental and first principle rates is satisfactory, in particular, where the experimental constants have less uncertainties. At 4 K the difference between theory and experiment is less than 25% for h_{02} and h_{13}.

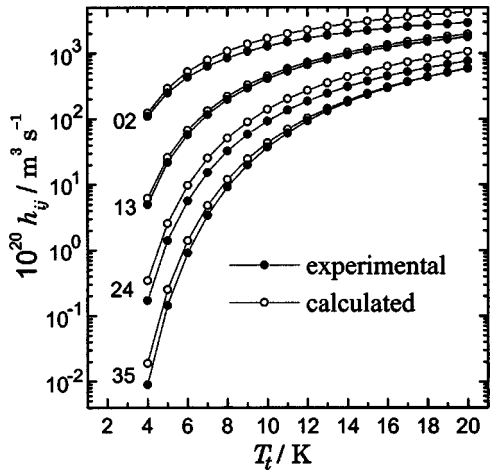

FIG. 6. Comparison between experimental and calculated rate constants h_{il} of N_2:He collisions.

From the theoretical point of view, the agreement between theory and experiment also represents a validation test for the PES used in the calculation. At these temperatures, $4<T<20$ K, N_2:He efficient collisions sample the bottom part of the wall as well as the well shape of the PES. The cross sections studied, even the σ_{35}, are mainly governed by the V_2 and V_4 anisotropic terms of the PES. So, the overall agreement between experimental and theoretical rates provides a reasonable validation of the leading anisotropic terms describing the low part of the PES.

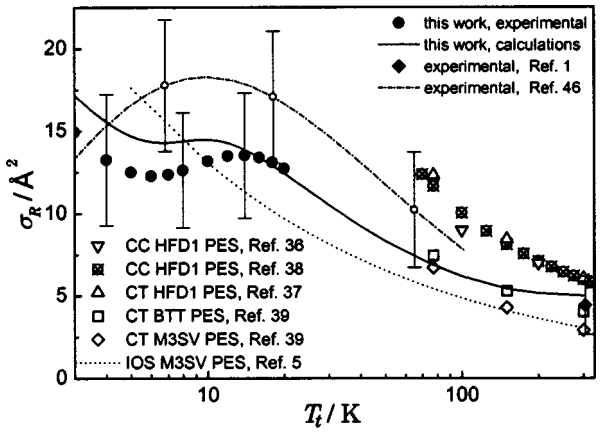

FIG. 7. Average rotational relaxation cross sections of N_2:He collisions vs translational temperature.

VII. AVERAGE ROTATIONAL RELAXATION CROSS SECTION

Having at our disposal rate constants, as an aside, we have calculated the average rotational relaxation cross section, σ_R, for the relaxation of the mean rotational energy of N_2 molecules in helium. In order to compare our results with the reports of Belikov *et al.*[44,5] we have used the same expression of the phenomenological cross section:[45]

$$\langle v\rangle \sigma_R(T) = (n_a \tau_R)^{-1} = \sum_j \sum_{i>j} h_{ij}(T) N_j^* \frac{(\epsilon_i - \epsilon_j)^2}{\langle \epsilon^2\rangle - \langle \epsilon\rangle^2}, \tag{18}$$

where $\langle \epsilon^n\rangle = \Sigma_j N_j^* \epsilon_j^n$ are the rotational energy moments and

$$N_j^* = \frac{g_j(2j+1)\exp(-\epsilon_j/k_B T)}{Q_R} \tag{19}$$

the equilibrium population of the $J=j$ rotational level at temperature T. For N_2 the nuclear statistical weight is $g_j = 1/3$ and $2/3$ for odd and even j, respectively; Q_R is the rotational partition function. Finally, n_a is the number density of He, and τ_R is the rotational relaxation time in collisions with helium atoms also related to the collision number $\zeta_{\rm rot}$ and the mean duration τ_c between collisions through the ratio: $\zeta_{\rm rot} = \tau_R/\tau_c$.[38]

The validity conditions of Eq. (18) have been discussed by Belikov *et al.*[45] A rough estimate, as performed by Aoiz *et al.*,[7] of the Massey type adiabaticity parameter tends to indicate that Eq. (18) is valid for temperatures down to a few Kelvin for this system.

Experimental values of σ_R for N_2:He collisions are scarce. Holmes *et al.*[1] measured this magnitude a long time ago, in a sound absorption experiment at a temperature of 304 K, and found a value of $\sigma_R = 4.2 \pm 1.6$ Å^2. In a more recent work, Aoiz *et al.*[46] used REMPI+TOF techniques to study the rotational relaxation in free jets of N_2 diluted in He and Ne. They found a value for the σ_R for the N_2:He system on the order of 15 Å^2 in the range $T = 5$–80 K.

The experimental results just mentioned are represented in Fig. 7, together with the σ_R derived from present work using Eq. (18). *Ortho*- and *para*-species have been combined in the appropriate ratio 2:1 to generate the n-N_2:He relaxation cross section. Indeed, *ortho*- and *para*-modifications of N_2 lead to very similar σ_R results for $T \geqslant 15$ K, while for $T \leqslant 10$ K σ_R can be estimated accurately by a two-level approximation.[47] Several theoretical results on N_2:He system,[5,36–39] obtained by various methods and with different PESs are also shown in Fig. 7. The differences between these PESs are well documented[18,29,30,43] and thus we will be brief. Since σ_R is greatly influenced by the inelasticities, the HFD1 PES of Fuchs *et al.*[42] is confirmed to be too anisotropic.[5,43,44] The classical trajectories (CT) calculations of Dickinson and Heck[39] using the BTT PES of Bowers *et al.*[48] are close to our calculated results where comparable. However their CT calculation using the multiproperty fitted M3SV PES of Gianturco *et al.*[49] agree with our calculate data only at 77 K. The BBT PES have similar anisotropy to the PES of Reid *et al.*,[18] both in the well depth and in the low repulsive part, while the M3SV PES becomes less anisotropic as the collision energy increases.

The n-N_2:He relaxation cross sections for temperatures $T \geqslant 15$ K can be described by the empirical equation:

$$\sigma_R(T) = a T^{-b}. \tag{20}$$

From our calculations we found $a = 39.6 \pm 1$ Å^2 and $b = 0.39 \pm 0.01$. Belikov *et al.*,[5] from their calculations within the framework of the infinite order sudden (IOS) approximation,[50] using the M3SV PES, found $a = 35.2$ Å^2 and $b = 0.43$ (see also Table 2 in Ref. 5 which provides fitted parameters for the other results displayed in Fig. 7). We consider the IOS approximation not well suited for this system because of the neglect of the energy level spacings, quite important due to the *ortho/para* separation at low temperatures. To corroborate this assertion IOS calculations were performed in the present work at various kinetic energies for the very first state-to-state cross sections. As shown in Fig. 5, IOS and CC results are quite different below 25 K. This limitation of IOS had already been mentioned by Thachuk and McCourt.[36]

VIII. SUMMARY AND CONCLUSIONS

A comprehensive study of the state-to-state RT rate constants for N_2:He collisions as a function of temperature ($3 < T < 20$ K) is presented in connection with first principles calculations of these quantities in a wider thermal range ($0 < T < 300$ K). In the thermal range where the comparison is possible good agreement has been found between experimental data and calculations. On one hand, the agreement represents a quality test for the N_2:He rate constants as well as for the N_2:N_2 rate constants determined in our previous paper[17] and, at the same time, it validates the experimental methodology. On the other hand, the agreement provides a validation for the potential energy surface[18] and for the dynamical method used in the calculations.

The experimental data presented here are susceptible to be improved. An extension of the method to expansions of N_2/He mixtures at different concentrations, and generated in different conditions of stagnation temperature, $T_0 > 300$ K, and/or stagnation pressure, may help improving the accuracy of the present results, increasing the number of constants determined and widening the thermal range to higher values.

ACKNOWLEDGMENTS

The authors are indebted to A. J. Thakkar for the use of the code to generate the N_2–He PES. Thanks are due to the Spanish MCYT for financial support of the experimental part of this work (Research Project No. BFM2001-2276).

[1] R. Holmes, G. R. Jones, N. Pusat, and W. Tempest, Trans. Faraday Soc. **58**, 2342 (1962).
[2] P. G. Kistemaker and A. E. de Vries, Chem. Phys. **7**, 371 (1975).
[3] A. E. Belikov, R. G. Sharafutdinov, and M. L. Strekalov, Chem. Phys. Lett. **231**, 444 (1994).
[4] M. Faubel and E. R. Weiner, J. Chem. Phys. **75**, 641 (1981).
[5] A. E. Belikov, R. G. Sharafutdinov, and A. V. Storozhev, Chem. Phys. **213**, 319 (1996).
[6] T. L. Manzely and M. A. Smith, J. Phys. Chem. **94**, 6930 (1990).
[7] F. J. Aoiz, T. Díez-Rojo, V. J. Herrero, B. Martínez-Haya, M. Menéndez, P. Quintana, L. Ramonat, I. Tanarro, and E. Verdasco, J. Phys. Chem. A **103**, 823 (1999).
[8] L. Abad, D. Bermejo, V. J. Herrero, J. Santos, and I. Tanarro, J. Phys. Chem. A **101**, 9276 (1997).
[9] L. Bonamy, J. Bonamy, D. Robert, B. Lavorel, R. Saint-Loup, R. Chaux, J. Santos, and H. Berger, J. Chem. Phys. **89**, 5568 (1988).
[10] T. G. A. Heijmen, R. Moszynski, P. E. S. Wormer, A. van der Avoird, A. D. Rudert, J. B. Halpern, J. Martin, W. B. Gao, and H. Zacharias, J. Chem. Phys. **111**, 2519 (1999).
[11] D. Bassi, A. Boschetti, S. Marchetti, G. Scoles, and M. Zen, J. Chem. Phys. **74**, 2221 (1981).
[12] T. E. Gough and R. E. Miller, J. Chem. Phys. **78**, 4486 (1983).
[13] A. E. Belikov and M. A. Smith, J. Chem. Phys. **110**, 8513 (1999).
[14] S. Liu, Q. Zhang, C. Chen, Z. Zhang, J. Dai, and X. Ma, J. Chem. Phys. **102**, 3617 (1995).
[15] R. G. Sharafutdinov, A. E. Belikov, M. L. Strekalov, and A. V. Storozhev, Chem. Phys. **207**, 193 (1996).
[16] G. O. Sitz and R. L. Farrow, J. Chem. Phys. **93**, 7883 (1990).
[17] A. Ramos, G. Tejeda, J. M. Fernández, and S. Montero, Phys. Rev. A **66**, 022702 (2002).
[18] J. P. Reid, A. J. Thakkar, P. W. Barnes, E. F. Archibong, H. M. Quiney, and C. J. S. M. Simpson, J. Chem. Phys. **107**, 2329 (1997).
[19] H. Rabitz and S. H. Lam, J. Chem. Phys. **63**, 3532 (1975).
[20] D. R. Flower and E. Roueff, J. Phys. B **32**, 3399 (1999).
[21] S. Montero, B. Maté, G. Tejeda, J. M. Fernández, and A. Ramos, in *Atomic and Molecular Beams: The State of the Art, 2000*, edited by R. Campargue (Springer, Berlin, 2000), p. 295.
[22] G. Tejeda, J. M. Fernández, and S. Montero, Appl. Spectrosc. **51**, 265 (1997).
[23] B. Maté, I. A. Graur, T. Elizarova, I. Chirokov, G. Tejeda, J. M. Fernández, and S. Montero, J. Fluid Mech. **426**, 177 (2001).
[24] A. Ramos, B. Maté, G. Tejeda, J. M. Fernández, and S. Montero, Phys. Rev. E **62**, 4940 (2000).
[25] See EPAPS Document No. E-JCPSA6-118-013310 for the experimental data n, T_r, T_t, and V, in expansions of N_2/He mixtures with molar fraction of N_2 $\alpha=0.47$ and $\alpha=0.076$. A direct link to this document may be found in the online article's HTML reference section. This document may also be reached via the EPAPS homepage (http://www.aip.org/pubservs/epaps.html) or from ftp.aip.org in the directory /epaps/. See the EPAPS homepage for more information.
[26] B. Maté, G. Tejeda, and S. Montero, J. Chem. Phys. **108**, 2676 (1998).
[27] S. DePaul, D. Pullman, and B. Friedrich, J. Phys. Chem. **97**, 2167 (1993).
[28] J. Fernández de la Mora and J. Rosell-Llompart, J. Chem. Phys. **91**, 2603 (1989).
[29] C.-H. Hu and A. J. Thakkar, J. Chem. Phys. **104**, 2541 (1996).
[30] L. Beneventi, P. Casavecchia, G. G. Volpi, C. C. K. Wong, F. R. W. McCourt, G. C. Corey, and D. Lemoine, J. Chem. Phys. **95**, 5827 (1991).
[31] D. R. Flower, G. Bourhis, and J. M. Launay, Comput. Phys. Commun. **131**, 187 (2000).
[32] J. M. Hutson and S. Green, MOLSCAT version 14, Collaborative Computational Project n6 of the UK Science and Engineering Research Council, 1994.
[33] P. McGuire and D. J. Kouri, J. Chem. Phys. **60**, 2488 (1974); R. T Pack, *ibid.* **60**, 633 (1974); R. Goldflam and D. J. Kouri, *ibid.* **66**, 542 (1977).
[34] B. R. Johnson, J. Chem. Phys. **69**, 4678 (1978).
[35] M. H. Alexander and D. E. Manolopoulos, J. Chem. Phys. **86**, 2044 (1987).
[36] M. Thachuk and F. R. W. McCourt, J. Chem. Phys. **95**, 4112 (1991).
[37] A. S. Dickinson and M. S. Lee, J. Phys. B **19**, 3091 (1986).
[38] G. C. Maitland, M. Mustafa, W. A. Wakeham, and F. R. W. McCourt, Mol. Phys. **61**, 359 (1987).
[39] A. S. Dickinson and E. L. Heck, Mol. Phys. **70**, 239 (1990).
[40] V. Vesovic, W. A. Wakeham, A. S. Dickinson, F. R. W. McCourt, and M. Thachuk, Mol. Phys. **84**, 553 (1995).
[41] F. R. W. McCourt, J. J. M. Beenakker, W. E. Kohler, and I. Kuscer, *Non-Equilibrium Phenomena in Polyatomic Gases* (Clarendon, Oxford, 1991), Vol. 2.
[42] R. R. Fuchs, F. R. W. McCourt, A. J. Thakkar, and F. G. Grein, J. Phys. Chem. **88**, 2036 (1984).
[43] F. A. Gianturco, N. Sanna, and S. Senna-Molinera J. Chem. Phys. **97**, 6720 (1992).
[44] A. E. Belikov and R. G. Sharafutdinov, Chem. Phys. Lett. **241**, 209 (1995).
[45] A. E. Belikov, A. I. Burshtein, S. V. Dolgushev, A. V. Storozhev, M. L. Strekalov, G. I. Sukhinin, and R. G. Sharafutdinov, Chem. Phys. **139**, 239 (1989).
[46] F. J. Aoiz, L. Bañares, V. J. Herrero, B. Martínez-Haya, M. Menéndez, P. Quintana, I. Tanarro, and E. Verdasco, Vacuum **64**, 417 (2002); Chem. Phys. Lett. **367**, 500 (2003).
[47] R. Schafer and R. G. Gordon, J. Chem. Phys. **58**, 5422 (1973).
[48] M. S. Bowers, K. T. Tang, and J. P. Toennies, J. Chem. Phys. **88**, 5465 (1988).
[49] F. A. Gianturco, M. Venanzi, R. Candori, F. Pirani, F. Vecchiocattivi, A. S. Dickinson, and M. S. Lee, Chem. Phys. **109**, 417 (1986); **113**, 166 (1987).
[50] R. Goldflam, S. Green, and D. J. Kouri, J. Chem. Phys. **67**, 4149 (1977).